Enhancing Power Efficiency and Grid Stability in Virtual Power Plants under Stochastic Uncertainties

Sajjad Khan[1*], M. Sajjad[2], A. Khan[3,] M. Ikram[4.] , M.Zafran[5]
[3, 4] School of Information Science and Engineering Southeast University, Nanjing, China
[1, 5] School of Electrical Engineering Southeast University, Nanjing, China
[2]Department of Electrical Engineering, Iqra National University, Peshawar, Pakistan
[*]corresponding author's email: muhammadsajjad0335@gmail.com

Abstract – *This study examines the integration of Virtual Power Plants (VPPs) to optimize grid operations using renewable energy, Energy Storage Systems (ESS), Electric Vehicles (EVs), and HVAC systems. It analyzes the effects of shading and weather uncertainties on solar power generation and employs adaptive control strategies to manage ESS and EV battery performance. The findings reveal that environmental factors, particularly shading and seasonal variations, significantly impact solar output. Adaptive control strategies effectively mitigate variability, improving energy storage performance and maintaining a stable State of Charge (SOC) in ESS and EV batteries. VPP integration enhances grid stability, optimizes power utilization, and improves system reliability. This research underscores the critical role of VPPs in addressing modern energy challenges by employing advanced energy management techniques. By adapting to uncertainties and optimizing resources, VPPs contribute to more efficient, reliable, and sustainable grid operations, supporting a resilient energy infrastructure.*

Keywords: *Electric vehicle, Energy storage, Grid reliability, Grid stability, Virtual power plant*

Article History
Received 23 October 2024
Received in revised form 3 December 2024
Accepted March 17 December 2024

I. Introduction

In the realm of contemporary energy management, the incorporation of VPPs signifies a fundamental change towards a more dynamic and robust grid infrastructure. VPPs involve a wide range of energy resources and technologies, such as PV systems [1], ESS [1] – [3], electric vehicles (EVs) [1],[4] – [7], and HVAC units [1],[8] – [9]. These components come together to create an advanced energy ecosystem capable of producing, storing, and distributing electricity in a highly efficient and adaptable manner. The incorporation of VPPs into established grid networks, like the IEEE 14 bus system, shows great potential for improving grid stability, reliability, and sustainability [1],[10] – [11].

At the core of VPP optimization is the utilization of sophisticated adaptive algorithms, among which adaptive control strategy stands out as a key tool for optimizing multi-objective functions [1],[12] – [13]. Adaptive control strategies empower VPPs to dynamically adapt energy generation, storage, and consumption tactics in accordance with changing grid conditions and user requirements. Through the reduction of operational expenses, maximization of power utilization, and mitigation of peak demand, adaptive control strategies boost the overall efficiency and efficacy of VPP operations. Furthermore, the incorporation of VPPs with adaptive [1],[13] aids in effectively coordinating various energy resources and technologies, ultimately enhancing grid flexibility and resilience. By employing these strategies and techniques, VPPs can dynamically adjust to fluctuations in grid conditions, minimize possible disruptions, and efficiently manage resource distribution in a timely manner.

In this all-encompassing investigation, we explore the complex interaction among VPP integration, employing adaptive control strategies, and grid management strategies. By conducting a thorough analysis of case studies and simulation findings, our goal is to clarify the transformative capacity of these technologies in shaping a sustainable and adaptable energy environment. Through an examination of the synergies between VPPs, adaptive control strategies, and grid infrastructure, our aim is to provide insights into the obstacles and possibilities linked to contemporary energy management practices, while also laying the groundwork for the advancement of more robust, effective, and environmentally friendly energy systems.

II. System Model

System modeling of VPP comprised of PV system, ESS, EVs and heat, ventilation and air conditioning (HVAC) and integration of VPP into electrical grid system with 14 buses.

A. Modeling of PV system

The PV system, which is considered a fundamental component of renewable energy, functions by producing electricity through the utilization of sunlight. In the context of VPPs, which serve as a collective platform for various distributed PV systems, there is an effective optimization of grid stability and reliability. Moreover, the PV systems play a significant role in the sustainable production of energy by efficiently harnessing solar energy, thus reducing the reliance on fossil fuels and effectively mitigating the environmental impacts associated with them. Within the framework of a VPP, the PV model takes into account a multitude of factors, including solar irradiance, temperature effects, shading analysis, inverter efficiency, and uncertainties as given by equation (1). Through the consideration and integration of these variables, the PV model is able to accurately predict the power output of the PV system, thereby facilitating its optimal integration within VPP frameworks. This optimal integration ultimately leads to enhanced management of renewable energy and a greater level of stability within the grid [1].

$$P(t)_{out} = P(t)_{max}[1 - \beta_T(T_t - T_{STC})] \times (1 - \alpha_{shading}) \times \eta_{inverter} \times G(t) \times \epsilon(t) \tag{1}$$

where, $P(t)_{max}$= maximum power of PV panel (in Watt), β_T= Temperature coefficient, T_{STC}= Standard test condition temperature, $\alpha_{shading}$= Shading effect, $\eta_{inverter}$= Inverter's efficiency, G(t)= Solar Irradiance, T(t)= Ambient temperature, $\varepsilon(t)$ = Stochastic uncertainty.

B. Modeling of ESS

ESS have a crucial and indispensable function in the realm of VPPs, as they enable the seamless and effective integration of renewable energy sources such as solar power. The ability to store surplus energy during times of low demand and subsequently supply it during periods of high demand is a vital aspect of ESS, as it greatly contributes to the overall stability and reliability of the power grid. Moreover, the inclusion of energy storage systems within VPPs not only enhances grid stability but also facilitates the optimal utilization of renewable resources, ensuring that they are harnessed to their fullest potential for the benefit of the entire system. The dynamics of an energy storage system within a VPP are effectively captured and represented by the equations (2) and (3), which play a crucial role in understanding and managing the system's behavior [2-3]. The equation (2) takes into account various factors such as charging/discharging efficiencies, operational costs, and stochastic uncertainties, all of which have a significant impact on the system's state of charge over time. By incorporating these elements, the equation (3) offers a comprehensive framework for optimizing energy storage operations, thereby contributing to the overall enhancement of grid stability and the efficient utilization of renewable energy within Virtual Power Plants. In essence, it serves as a fundamental pillar in achieving the goals of maximizing the potential of energy storage systems and promoting sustainable energy practices in VPPs [1].

$$\frac{dE(t)_{ESS}}{dt} = \eta_{chargig} \times P(t)_{charging} - \frac{1}{\eta_{discharging}} \times P(t)_{discharging} \tag{2}$$

$$E(t+dt)_{ESS} = E(t)_{ESS} + \frac{dE(t)_{ESS}}{dt} \times dt + \varepsilon(t) \tag{3}$$

where, $\frac{dE(t)_{ESS}}{dt}$ = change of SOC with respect to time t, $\eta_{charging}$= charging efficiency, $\eta_{discharging}$= Discharging efficiency, $P(t)_{charging}$= charging power at time t, $P(t)_{discharging}$= Discharging power at time t, $\varepsilon(t)$= stochastic uncertainty in SOC dynamics.

C. System model of EVs

EVs have a crucial and indispensable role to play in the functioning of VPPs, as they provide immense value in terms of grid flexibility and demand-side management. By incorporating EVs into the power grid, a multitude of benefits become accessible, including the ability to dynamically balance the load, mitigate peak energy demand, and enhance storage capacity. Moreover, the integration of EVs represents a significant step towards the integration of renewable energy sources, as they contribute to the seamless assimilation of these sources into the grid. In doing so, they not only bolster grid stability but also pave the way for optimal cost management, thereby fostering the development of sustainable energy systems that are capable of effectively reducing carbon emissions. Equation (4) is used to calculate the charging power of EVs with power fluctuation $\delta(t)_{charging}$ and stochastic uncertainty $\varepsilon(t)_{charging}$. Equation (5) is used to calculate the discharging power of EVs with power fluctuation $\delta(t)_{discharging}$ and stochastic uncertainty $\varepsilon(t)_{discharging}$ while equation (6) is used to show the dynamic nature of SOC of the batteries of EVs. The equations from (4) – (6) accurately represent the dynamic behavior of EVs in a VPP, are crucial for analyzing the interactions between EVs and the grid [4] – [7]. They consider uncertainties, power fluctuations, and operational constraints, enabling the effective integration of EVs into grid operations for optimized renewable energy utilization and minimized disruptions. These equations also provide insights into the impact of EV charging and discharging patterns on grid performance, making them valuable for policymakers, grid operators, and researchers in developing strategies for enhanced EV integration and utilization within grid operations, advancing sustainable energy and smart grid technologies [1].

$$P(t)^{EV}_{Charging} = \left[P^{max}_{charging}, \left(P(t)_{demand} - P(t)_{generated}\right)\right] + \varepsilon(t)_{charging} + \delta(t)_{charging} \tag{4}$$

$$P(t)^{EV}_{disCharging} = \left[P^{max}_{discharging}, \left(P(t)_{generated} - P(t)_{demand}\right)\right] + \varepsilon(t)_{discharging} + \delta(t)_{discharging} \tag{5}$$

$$E(t+dt)_{EV} = E(t)_{EV} + \left(\eta_{charging} \times P(t)_{charging} - \frac{1}{\eta_{discharging}} \times P(t)_{discharging}\right) \times dt \tag{6}$$

where, $P(t)^{EV}_{Charging}$ = charging power of EVs at time t, $P(t)^{EV}_{disCharging}$ = Discharging power if EVs at time t, $E(t)_{EV}$= state of charge of EVs at time t, $E(t+dt)_{EV}$= Dynamic state of charging of EVs , $\eta_{charging}$= charging efficiency of EVs, $\eta_{discharging}$= Discharging efficiency of EVs, $\varepsilon(t)_{charging}$= stochastic uncertainty of charging at time t, $\delta(t)_{charging}$= power fluctuation of charging of EVs at time t, $\varepsilon(t)_{discharging}$= Discharging uncertainty at time , $\delta(t)_{discharging}$= power fluctuation of discharging of EVs at time t.

D. Model of HVAC

HVAC systems play a crucial role in VPPs as they are essential for maintaining optimal indoor comfort levels while simultaneously optimizing energy consumption in an efficient manner. These systems are intelligently integrated with smart controls, thereby providing demand response capabilities that greatly contribute to grid stability and effective peak load management. The integration of HVACs within VPPs not only enhances the overall efficiency of the power plant but also results in significant reductions in energy costs and environmental impact. Furthermore, the utilization of these systems ensures that the comfort and wellbeing of building occupants are consistently prioritized and upheld, thereby creating a harmonious balance between energy optimization and occupant satisfaction. This particular model takes into consideration the presence of stochastic uncertainties in the power consumption of HVAC systems, thereby enabling more precise predictions and enhanced management of energy resources within the VPP. By doing so, it facilitates the implementation of optimized control strategies that aim to maintain optimal indoor comfort levels while simultaneously minimizing energy costs and the overall impact on the grid. Equation (7) is employed to compute the power consumption of the HVAC system, while equation (8) is utilized to determine the dynamic nature of the indoor temperature within said system. Furthermore, equation (9) serves as the threshold or limit for power consumption, establishing a benchmark that ensures efficient usage of energy [1],[8] – [9].

$$P(t)_{HVAC} = \alpha \times (T_{set} - T(t)_{indoor}) + \varepsilon(t)_{HVAC} \tag{7}$$

$$T(t+dt)_{indoor} = T(t)_{indoor} + \beta(T(t)_{outdoor} - T(t)_{indoor}) \times dt \tag{8}$$

$$0 \le P(t)_{HVAC} \le P_{max} \tag{9}$$

where, $P(t)_{HVAC}$= Power consumption by HVAC in time t, α= coefficient representing efficiency and capacity of HVAC, $\varepsilon(t)_{HVAC}$= Stochastic uncertainty varying with time t, $T(t)_{indoor}$= Indoor temperature, $T(t)_{outdoor}$= Outdoor temperature, β= coefficient representing thermal characteristics, $T(t+dt)_{indoor}$= Dynamic nature of indoor temperature.

E. Integration of VPP into IEEE 14 bus system

The incorporation of a VPP that consists of PV systems, ESS, EVs, and HVAC units into a 14-bus electrical grid system that caters to both commercial and residential loads is of immense significance. This integration brings about a multitude of benefits by effectively managing and harnessing various energy resources, thereby enhancing the flexibility, stability, and efficiency of the grid. By effectively utilizing renewable energy sources, storage capabilities, and demand-side management, the VPP optimizes energy consumption, reduces dependency on fossil fuels, and effectively addresses grid congestion issues. This seamless integration paves the way for the establishment of a more sustainable and resilient energy infrastructure, which in turn supports the transition towards a grid ecosystem that is both cleaner and more intelligent [10] – [11]. After integrating VPP into electrical grid system, the total power at the bus to which VPP is connected, can be calculated by using equation (10) [1].

$$P^{VPP}_{Bus} = P_{PV} + \Delta P_{ESS} + \Delta P_{EVs} + P_{HVAC} \tag{10}$$

where, $\Delta P_{ESS} = P_{charging} - P_{discharging}$, and $\Delta P_{EVs} = P_{charging} - P_{discharging}$. The assessment of the Impact Analysis involves the examination and evaluation of the alterations in power distribution at individual electrical substations before and after the integration of the VPP. This evaluation is denoted as ΔP^{VPP}_{Bus}. Equation (11) is used to show the impact analysis of the integration of VPP into electrical grid system [1].

$$\Delta P^{VPP}_{Bus} = P^{with\,VPP}_{bus} - P^{without\,VPP}_{bus} \tag{11}$$

Quantifying these changes is essential for comprehending the impact of VPP on electrical grid dynamics and optimizing grid operations in changing energy landscapes.

III. Evaluation of Virtual power plant

The evaluation of VPP comprised of the evaluation if multi-objective function optimization adaptive control strategies, different constraints used by VPP, evaluation metrics and novelty of the research study.

A. Multi-objectives function

In order to apply adaptive control strategies on virtual power plant when integrated it into electrical grid system, multi-objective function would be used to minimize the total cost, maximize the power utilization, reducing maximum demand, and enhancing grid stability and reliability [1], [12] – [13]. The multi-objective function J can be defined as illustrated by equation (12).

$$J = w_1 \times C + w_2 \times U_p - w_3 \times D_{max} - w_4 \times S_{grid} - w_5 \times R_{grid} \quad (12)$$

where, J is the objective function, w_1, w_2, w_3, w_4, and w_5 are the weighting factors and used to show the importance of each objective, C is the total cost of VPP operation and it is actually the sum of generation cost $C_G(t)$ including fixed generation $C_{fix}(t)$ and variable generation $C_{var}(t)$ cost at a particular period of time t as given by equation (13), total energy storage cost $C_{ES}(t)$ including operational cost $C_{op}(t)$ and degradation cost $C_{deg}(t)$ at particular duration of time t as given by equation (14), Total energy distribution cost $C_{dist}(t)$ including total cost of transmission losses $C_{loss}(t)$ at a particular period of time as given by equation (15) and the cost associated with managing uncertainties $C_{uncert}(t)$ in generation $C_{res}(t)$ and forecasting $C_{forcast}(t)$ as given by equation (16) [1].

$$C_{gen}(t) = \sum_{i=1}^{N_{gen}} (C_{fix}^i(t) + C_{var}^i(t)) \quad (13)$$

$$C_{ES}(t) = \sum_{j=1}^{N_{ES}} (C_{op}^j(t) + C_{deg}^j(t)) \quad (14)$$

$$C_{dist}(t) = \sum_{k=1}^{N_{dist}} (C_{loss}^k(t)) \quad (15)$$

$$C_{uncert}(t) = \sum_{l=1}^{N_{uncert}} (C_{res}^l(t) + C_{forcast}^l(t)) \quad (16)$$

By combining equation (13), (14), (15) and (16), we can get total cost of VPP operation as shown by equation (17). Where N_{gen} is the total number of generation units, N_{ES} is the total number of storage units, N_{dist} is the total number of distribution units, and N_{uncert} is the total number of units associated with uncertainty cost.

$$C = \sum_{i=1}^{N_{gen}} \sum_{j=1}^{N_{ES}} \sum_{k=1}^{N_{dist}} \sum_{l=1}^{N_{uncert}} (C_{gen}^i(t) + C_{ES}^j(t) + C_{dist}^k(t) + C_{uncert}^l(t)) \quad (17)$$

U_P in equation (12) is used to show total power utilization. U_p is a measure of how effectively the VPP is able to generate and distribute power to meet demand. Equation (18) for U_p in a VPP considers the total power generated $P_{gen}(t)$, stored $P_{ES}(t)$, distribute $P_{dist}(t)$, and potentially lost due to inefficiencies $P_{loss}(t)$.

$$U_p(t) = \frac{P_{demand}(t)}{P_{gen}(t)+P_{ES}(t)+P_{dist}(t)+P_{loss}(t)} \quad (18)$$

D_{max} is used to show maximum demand of electrical grid system and can be given by equation (19) while $D_{max,VPP}$ is used to show maximum demand after incorporating VPP as given by equation (20). Where $P_{load}(t)$ is the power of load connected to electrical grid system.

$$D_{max} = P_{load}(t) \quad (19)$$

$$D_{max,VPP} = (P_{load}(t) - (P_{gen}(t) + P_{ES}(t) + P_{dist}(t) + P_{loss}(t)) \quad (20)$$

S_{grid} is the stability of electrical grid system is dependent upon power balance $P_{balance}(t)$ as given by equation (21), frequency deviation $\Delta f(t)$ as given by equation (22) and voltage stability which is influenced by reactive power balance $Q_{balance}(t)$ as shown by equation (23), whereas, the stability of grid system is given by equation (24).Where, H is the inertia constant of grid system.

$$P_{balance}(t) = P_{grid}(t) + P_{VPP}(t) - \left(P_{load}(t) + P_{loss}(t)\right) \quad (21)$$

$$\Delta f(t) = \frac{1}{2H}\int_0^t P_{balance}(t)dt \quad (22)$$

$$Q_{balance}(t) = Q_{grid}(t) + Q_{VPP}(t) - \left(Q_{load}(t)\right) \quad (23)$$

$$S_{grid} = \{P_{balance}(t) \approx 0 ; \quad for\ 100\%\ stability\ \Delta f(t) \approx 0; \quad for\ zero\ frequency\ deviation\ Q_{balance}(t) \cong 0; \quad for\ voltage\ stability \quad (24)$$

R_{grid} is the reliability of electrical grid system as indicated by equation (25).

$$R_{grid} = \frac{\int_0^T (P_{gen}(t)+P_{ES}(t)+P_{dist}(t)+P_{loss}(t))dt}{\int_0^T P_{load}(t)dt} \quad (25)$$

In multi-objectives function, J_2 is given by equation (26). Where P_{bus} is the power of bus to which aggregator is connected and X is the load connected to bus.

$$J_2 = -\left|P_{bus} - \left(4 \times P_{agg} + \sum X\right)\right| \quad (26)$$

J_3 is given by equation (27), which is based on maximum energy trading position.

$$J_3 = -max(X_i) \quad (27)$$

J_4 is another objective of multi-objectives function which shows the function controlling the grid stability and grid reliability and it can be given by equation (28).

$$J_4 = -(S_{grid}, R_{grid}) \tag{28}$$

B. Different constraints used by VPP

Different constraints used in evaluation of virtual power plant integrating into electrical grid system for optimal scheduling and bidding strategies are given below.

1) Total power generation constraint

The total power generation constraint of VPP integrating into electrical grid system can be illustrated with help of equation (29). Where, P(t) is the power generated by i^{th} VPP at time t, and P_{max} is the maximum possible generated power.

$$\sum_{i=1}^{N} P(t)_i \leq P_{max} \quad \forall t \tag{29}$$

2) Individual component constraints

The individual component constraints are charging and discharging constraint of energy storage system as shown by equation (30) and (31), charging and discharging constraints of electrical vehicles as illustrated by equation (32) and (33) and the constraint of power utilization of HVAC is given by equation (34).

$$ESS\ charging\ rate: \quad P(t)_{ESS_{charging}} \leq P_{max(ESS)_{charging}} \tag{30}$$

$$ESS\ discharging\ rate: P(t)_{ESS_{discharging}} \leq P_{max(ESS)_{discharging}} \tag{31}$$

$$EV\ charging\ rate: \ P(t)_{EV_{charging}} \leq P_{max(EV)_{charging}} \tag{32}$$

$$EV\ discharging\ rate: P(t)_{EV_{discharging}} \leq P_{max(EV)_{discharging}} \tag{33}$$

$$Power\ limit\ of\ HVAC: \quad P(t)_{HVAC} \leq P_{HVAC_{max}} \tag{34}$$

3) Optimal scheduling strategy

In optimal scheduling strategies parameters, $S^{(t)}$ is used to show the optimal scheduling parameters for each particle at iteration time t and $s_1^{(t)}$ is the parameter for charging rate of ESS, $s_2^{(t)}$ is the parameter for discharging rate of ESS, $s_3^{(t)}$ is the parameter for storage level of ESS, $s_4^{(t)}$ is the parameter for demand level of EVs, $s_5^{(t)}$ is the parameter for demand level of HVAC and $s_6^{(t)}$ is the amount of surplus power if available. Equation (35) is used to show the optimal scheduling strategy of VPP in the framework of the solution bi-level stochastic optimization problem using adaptive control strategy.

$$S^{(t)} = \{s_1^t, s_2^t, s_3^t, s_4^t, s_5^t, s_6^t\} \tag{35}$$

4) Bidding strategy

In optimal scheduling strategies parameters, $B^{(t)}$ is used to show the bidding strategy parameters for each particle at iteration time t and $b_1^{(t)}$ is the parameter for bid prices, $b_2^{(t)}$ is the parameter for quantities of bid strategies, and $b_3^{(t)}$ is the parameter for bid threshold. Equation (36) is used to show the bidding strategy of VPP in the framework of the solution bi-level stochastic optimization problem using adaptive control strategy.

$$B^{(t)} = \{b_1^t, b_2^t, b_3^t\} \tag{36}$$

5) Energy trading position

Energy trading position is basically the position of the particle of adaptive control strategy, which represent the energy trading decisions, and used to specify that how much energy has to buy or sell at time iteration t at different scenarios i=1,2,3,…..N. Equation (37) is used to show position of particle $x_i^{(t)}$ the energy trading position for different scenarios of bidding. Where, x_N^t is the energy trading position of a particle at N number of scenario.

$$X_i^{(t)} = \{x_1^t, x_2^t, x_3^t, \ldots\ldots, x_N^t\} \tag{37}$$

C. Structure algorithm of Multi-objectives function optimization

Structured algorithms offer a methodical way to address intricate problems with multi-objective functions by dividing tasks into distinct, step-by-step processes. They improve the clarity, effectiveness, and manageability of code, assisting in comprehending and applying different adaptive techniques. Through arranging the flow of logic and data, structured algorithms support the adaptive procedure, allowing for the simultaneous reduction or increase of various goals in a harmonized approach. Table I shows structure algorithm of multi-objective function of VPP.

TABLE I
STRUCTURE ALGORITHM OF MULTI-OBJECTIVE FUNCTION OF VPP

Structure algorithm of multi-objective function of VPP
Start: 1. Initialization of input parameters: $N_{Particle}$, $N_{iteration}$, $N_{variable}$, $C_{panel\_per\_watt}$, W_{panel}, $C_{ess\_per\_Wh}$, $C_{EV\_per\_Wh}$ 2. Define multi-objective function: $J_1 = w_1 \times C + w_2 \times U_p - w_3 \times D_{max} - w_4 \times S_{grid} - w_5 \times R_{grid}$ $J_2 = -\lvert P_{bus} - (4 \times P_{agg} + \Sigma x)\rvert$ $J_3 = -\max(x_1)$ $J_4 = -(S_{grid}, R_{grid})$ 3. Define constraints function: $f_{constraints}(x) = \Sigma x - P_{bus}$ 4. initialization: $P_{position}$=Rand($N_{particles}$, $N_{variables}$); $P_{velocity}$=zeros($N_{particles}$, $N_{variables}$); 5. main loop: For iter=1:$N_{iteration}$ Evaluate J_i for each particles Update particle velocity and position Clamps positions within the bounds

End
6. Evaluate grid stability and reliability
[S_{grid}, R_{grid}]=simulate_grid(x,busdata, linedata);
Optimized solution and metrics
7. Display J_i the multi-objective functions
End

IV. Results and Discussions

This section deals with the analysis of a VPP involves a detailed examination of various components such as PV systems, ESS systems, EVs, and HVACs, focusing on their unique characteristics and functions within the VPP framework for efficient grid operation. In Fig. 1, a line graph shows the solar plant's power output in winter under various shading and weather uncertainty scenarios. Blue represents 10% shading with 0% uncertainty, red shows 10% shading with 10% uncertainty, black represents 50% shading with 10% uncertainty, green shows 50% shading with 50% uncertainty, yellow represents 80% shading with 50% uncertainty, and cyan illustrates 80% shading with 80% uncertainty. The graph demonstrates that as shading and uncertainty increase, maximum output power decreases, highlighting the significant impact of these factors on solar power generation.

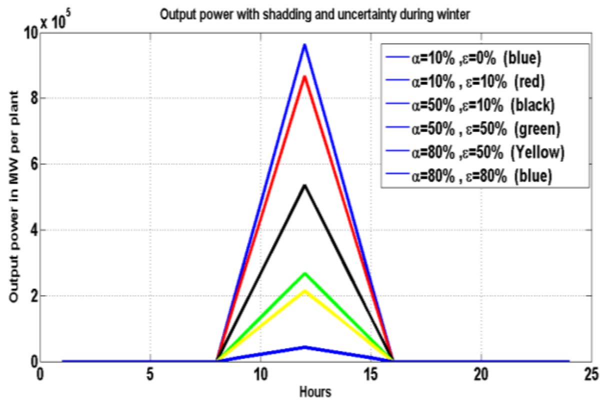

Fig. 1: Output power with shading effect and weather uncertainty generated during winter

Fig. 2 shows how a solar plant's output power during summer is affected by shading and weather uncertainty. Under ideal conditions (10% shading, 0% uncertainty), the maximum power reaches 1.5 MW (blue line). As shading and uncertainty increase, output power drops significantly, with 80% shading and 80% uncertainty reducing it to 0.1 MW (cyan line). This highlights the strong influence of these factors on summer solar performance. Despite abundant sunlight, shading and weather variability still affect efficiency, underscoring the importance of site selection, panel alignment, and advanced forecasting for optimal performance.

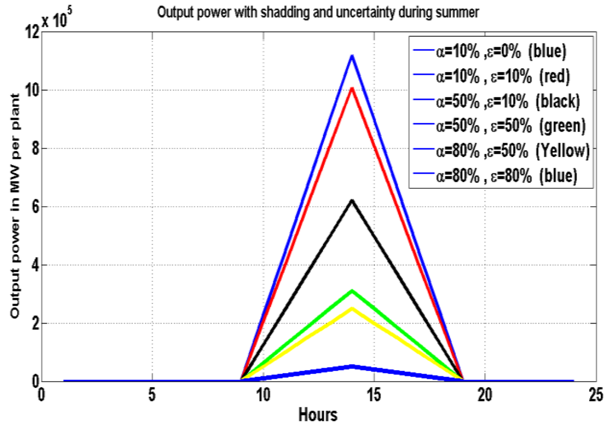

Fig. 2: Output power with shading effect and weather uncertainty generated during summer

Fig. 3 and 5 illustrate the hourly charging power fluctuations of the Energy Storage System (ESS) in summer due to stochastic uncertainty and adaptive control strategies. In Fig. 3, the red line shows steady charging around 1MW during peak solar irradiance, while the blue line highlights variability, with instances of zero power input caused by uncertainties like grid connections and market dynamics. Fig. 4 and 5 depict similar patterns in winter. Adaptive control in Fig. 5 manages uncertainties, aligning with the stable red line in Fig. 3 and 4, showcasing the strategy's effectiveness in optimizing energy use and ensuring reliable ESS performance under changing conditions.

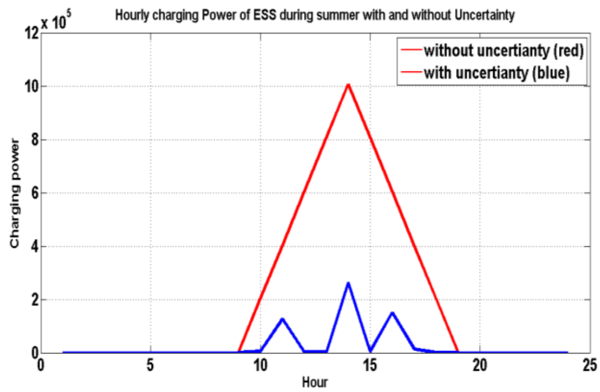

Fig. 3: Charging power of ESS with and without stochastic uncertainty during summer

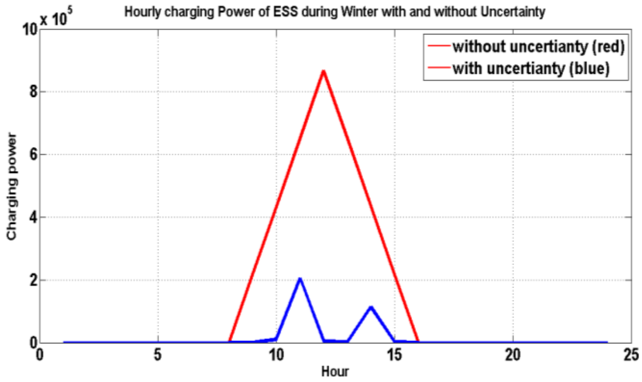

Fig. 4: Charging power of ESS with and without uncertainty during winter

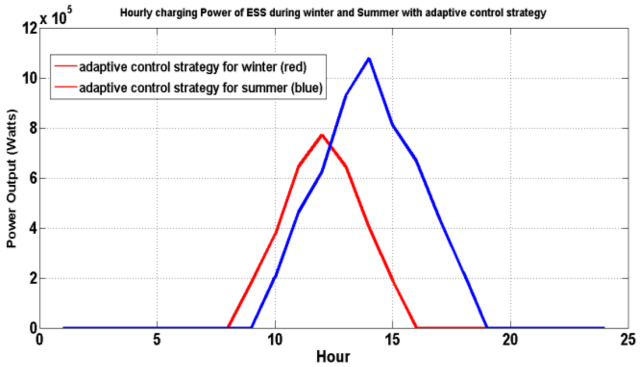

Fig. 5: Charging power of ESS with adaptive control strategy during summer and winter

Fig. 6, 7, and 8 compare the impact of stochastic uncertainty and adaptive control strategies on the dynamic State of Charge (SOC) of the Energy Storage System (ESS) under summer conditions. In Fig. 6, the red line shows a predictable SOC, charging to 95% during peak solar hours and discharging to 38% by the 24th hour, while the blue line shows fluctuations from 2% to 16% due to uncertainties like grid variability. Fig. 7 follows a similar trend, reaching 65%, while Fig. 8, with adaptive control, stabilizes SOC, peaking at 92%. Adaptive control minimizes uncertainties, improving SOC management and system efficiency.

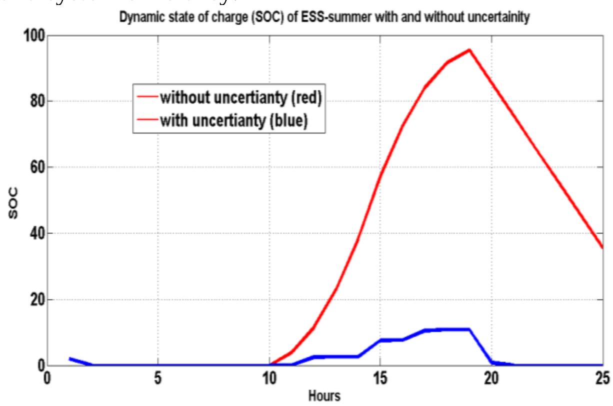

Fig. 6: Dynamic state of charge of ESS with and without stochastic uncertainty during summer

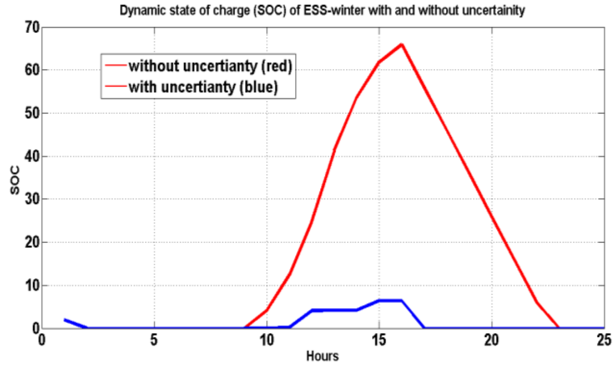

Fig. 7: Dynamic state of charge of ESS with and without stochastic uncertainty during winter

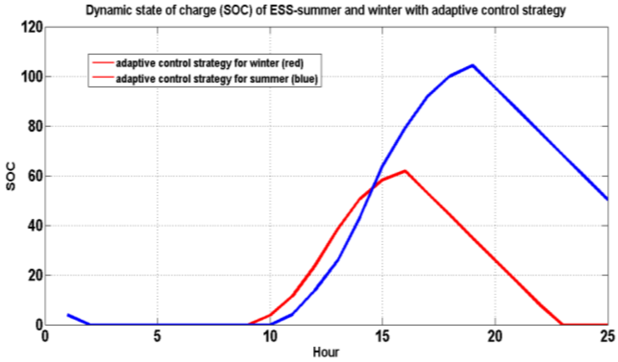

Fig. 8: Dynamic state of charge of ESS with application of adaptive control strategy during summer and winter

Fig. 9 illustrates the charging demand of EVs under stochastic influences like battery degradation and energy market prices during summer and winter. Initially, the demand is low at 0.1MW but rises to 0.9MW–1MW between hours 13 and 17, likely due to peak EV usage or energy price fluctuations. Fig. 10 shows the effect of applying an adaptive control strategy (PID) in both seasons. Charging power peaks between hours 11 and 14 in winter and 13 and 17 in summer, maintaining levels around 0.6MW–0.7MW, demonstrating the strategy's effectiveness in optimizing energy use and managing dynamic demand.

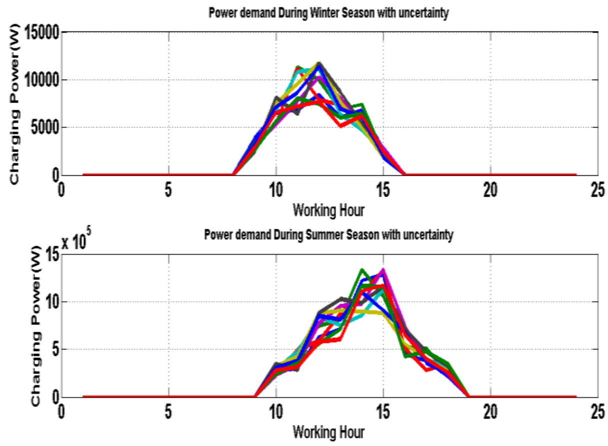

Fig. 9: Charging demand of EVs with stochastic uncertainty during summer and winter
summer and winter

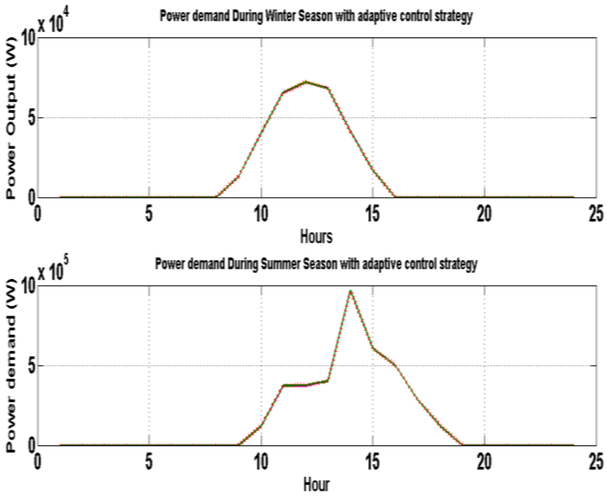

Fig. 10: Charging demand of EVs with adaptive control strategy during summer and winter

Fig. 11 highlight the dynamic SOC in EV batteries influenced by stochastic uncertainty. In winter, SOC stabilizes at around 10% before discharging, while in summer, it peaks at a slightly higher level. Fig. 12 demonstrate the effectiveness of adaptive control, particularly the PID controller, in maintaining consistent SOC levels. By dynamically adjusting charging rates, the adaptive strategy optimizes SOC, enhancing battery efficiency and lifespan. In both seasons, SOC approaches 100% during charging and transitions smoothly to discharging, showcasing the reliability of adaptive control in managing EV battery performance under varying conditions.

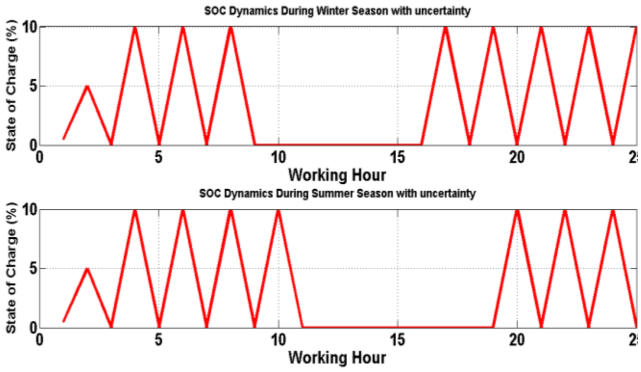

Fig. 11: Dynamic state of charge of the batteries of EVs with consideration of Stochastic uncertainty during summer and winter

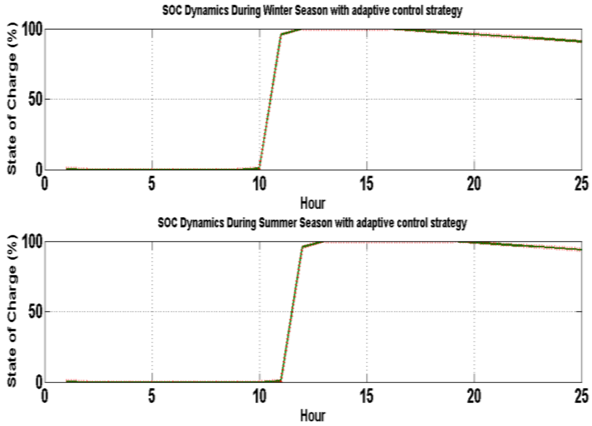

Fig. 12: Dynamic state of charge of Batteries of EVs with application of adaptive control strategy during summer and winter

Fig. 13 illustrates the indoor temperature fluctuations over a 24-hour period, starting at 46°C and stabilizing at 32°C. The most notable change occurs between the tenth and fifteenth hour, where the temperature drops rapidly by 10°C. This decrease likely result from the activation of cooling systems demonstrating the effectiveness of temperature regulation in enhancing indoor comfort. The rapid cooling phase highlights the importance of efficient cooling strategies to maintain a comfortable living environment.

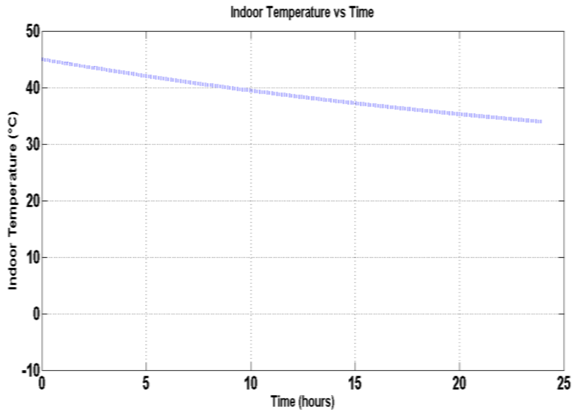

Fig. 13: Dynamic nature of indoor temperature with passage of time

A. Case Analyses

In this case study, we use adaptive control strategy to optimize a VPP integration into the grid, aiming to reduce operational costs and improve power utilization. By lowering peak demand, we enhance overall efficiency, stability, and reliability, advancing a robust energy infrastructure to meet modern demands.

Case 1: Cost minimization of the operation of VPP

A thorough method was used to optimize cost operations of a VPP within the electrical grid system, which involved employing advanced analytics, VPP to efficiently manage resources and reduce operational costs. The comparison of actual and optimized VPP costs using adaptive algorithm over 20 iterations reveals that the optimized cost initially exceeds the actual cost, showcasing VPPs efficiency. Between iterations 2 and 4, the costs converge, indicating a potential plateau. At iteration 4, both costs reach zero, reflecting an effective setup. Later, negative costs may arise from penalties or numerical precision issues. The optimized cost's drop to -1 x 10^7 PKR by iteration 15, matched by the actual cost at iteration 16, suggests algorithmic tendencies or local minimum convergence, as shown in Fig. 14. This analysis highlights VPP's impact on cost efficiency and the importance of monitoring cost patterns for improving VPP operations.

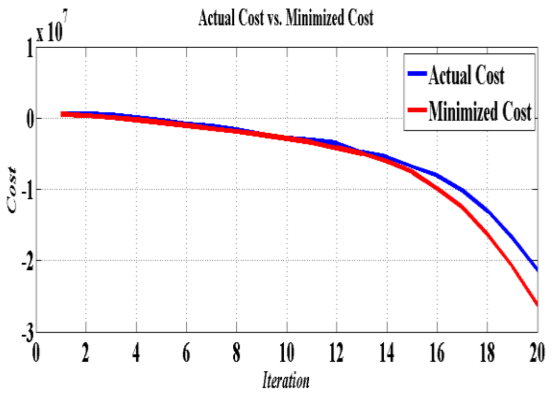

Fig. 14: operation cost minimization of electrical grid system incorporating VPP

Case 2: maximizing power utilization of VPP

Enhancing a cutting-edge VPP involves optimizing stored, utilized, and distributed power by integrating sustainable energy sources. Fig. 15 illustrates VPP's impact on the electrical grid system, highlighting a significant decrease in stored power from 37MW to 5MW, indicating better energy utilization. While consumed power rises slightly to 10MW, total delivered power surges to 74MW, demonstrating VPP's effectiveness in resource allocation and power delivery. This increase underscores VPP's transformative role in improving the efficiency and sustainability of the electrical grid system.

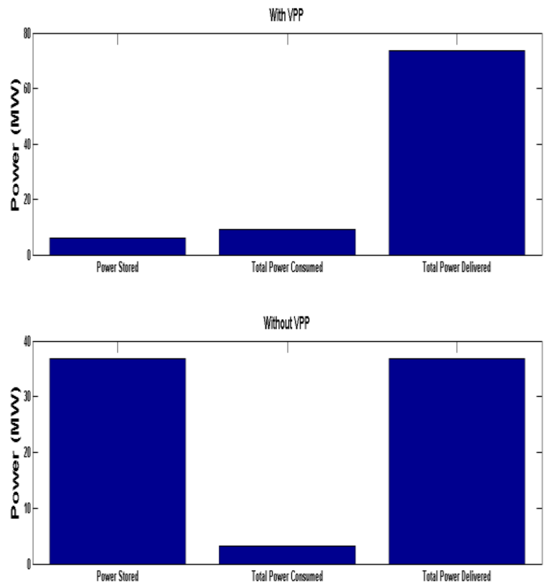

Fig. 15: Maximization of the utilization of power using VPP

Case 3: Grid stability and reliability

Fig. 16 compares grid stability and reliability under two scenarios: "Grid stability simple" and "Grid stability Vpp." The x-axis represents the scenarios, while the y-axis shows the percentage levels of grid stability and reliability. In the simple scenario, grid stability is relatively high at 80%, but in the Vpp scenario, it increases significantly to 95%, indicating a notable improvement. For grid reliability, the simple scenario stands at 20%, with a modest increase to 25% in the Vpp scenario. While the Vpp approach greatly enhances grid stability, its impact on reliability is less pronounced. This suggests that the Vpp method is particularly effective for boosting grid resilience and robustness, reducing blackouts, improving system efficiency, enhancing power quality, and making the grid more resilient to external disturbances like extreme weather and cyber-attacks.

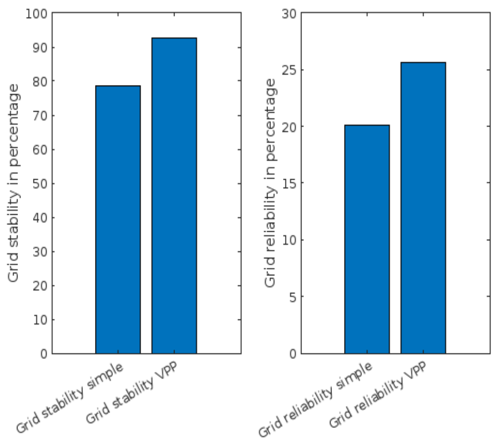

Fig. 16: Grid stability and reliability integrating VPP

Case 4: Optimal scheduling of VPP in electricity market

The comparison of the upper and lower subplots in Fig. 17 reveals insights into the impact of bi-level stochastic optimization on VPP scheduling within the electricity market. The upper subplot, representing scheduling without bi-level stochastic optimization, shows limited optimal behavior, indicating challenges in capturing uncertainties like demand fluctuations and price volatility. In contrast, the lower subplot, utilizing bi-level stochastic optimization, demonstrates improved scheduling effectiveness by addressing market uncertainties through probabilistic forecasting.

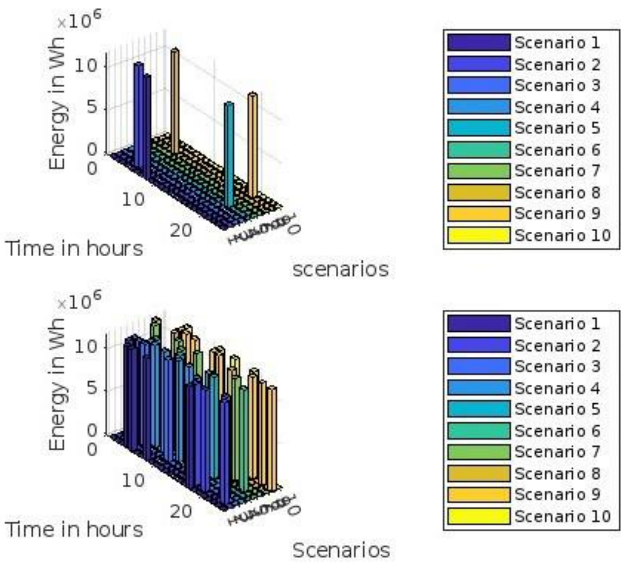

Fig. 17: Optimal scheduling of VPP in electricity market with and without bi-level stochastic optimization

Case 5: Bidding strategy of VPP in electricity market

The comparison between the upper and lower subplots of Fig. 18 illustrates a clear disparity in the revenue results of the bidding strategy employed by the Virtual Power Plant in the electricity market, with and without the utilization of bi-level stochastic optimization. In the upper subplot, where bi-level stochastic optimization is not utilized, most scenarios generate revenue below 1 x 10^4 USD. This suggests that the deterministic bidding strategy may face challenges in effectively adapting to and exploiting the dynamic market conditions and uncertainties, leading to suboptimal revenue generation. On the other hand, in the lower subplot, which incorporates bi-level stochastic optimization, the revenue outcomes for the majority of scenarios exceed 1 x 10^5 USD. This notable enhancement highlights the transformative effect of bi-level stochastic optimization in improving the VPP's bidding strategy. Through the integration of probabilistic forecasting, risk management, and advanced optimization techniques, bi-level stochastic optimization empowers the VPP to dynamically adjust its bidding decisions in accordance with evolving market dynamics and uncertainties. This adaptive approach not only maximizes revenue potential but also reinforces the VPP's resilience and competitiveness within the electricity market landscape.

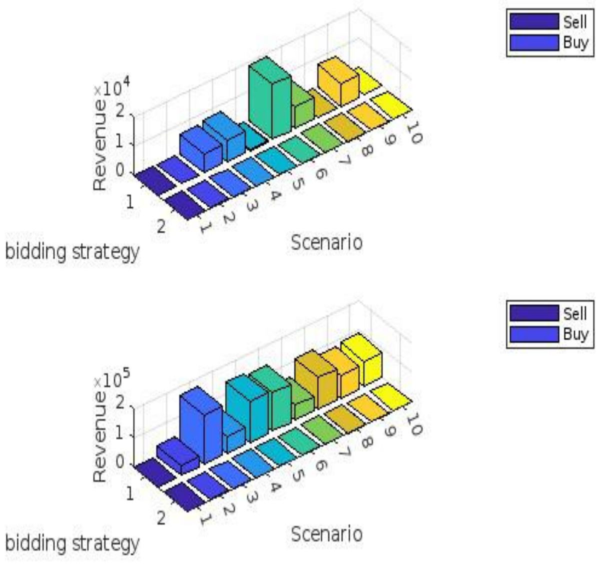

Fig. 18: Bidding strategy of VPP in electricity market with and without bi-level stochastic optimization

Bi-level stochastic optimization benefits from its ability to consider uncertainties in market parameters and system constraints, optimizing strategic decisions at the upper level and utilizing probabilistic forecasts at the lower level. The approach enables VPPs to balance risk and reward effectively, leading to adaptive scheduling solutions resilient to market uncertainties. Additionally, the bi-level stochastic optimization framework further enhances performance by efficiently exploring complex optimization problems, making it suitable for addressing the challenges faced by VPPs in the electricity market. Ultimately, the comparison highlights the crucial role of bi-level stochastic optimization in enhancing VPP scheduling performance by maximizing revenue, minimizing risk, and improving overall efficiency in dynamic market environments.

The frequency distribution of power sold by the Virtual Power Plant to the electricity market, as shown in Fig. 18, provides important insights into the distribution patterns and market behavior of the VPP's power sales. The distribution reveals various trends and anomalies in the frequency of power sales across different power output ranges. Initially, the distribution shows a fairly even pattern, with consistent frequencies of power sold between 0 and 2.5 MW, indicating steady market demand within this range. However, changes in the distribution become apparent as the power output exceeds 2.5 MW. Specifically, there is an increase in the frequency of power sales between 2.5 and 3 MW, followed by a decrease between 3 and 4 MW, suggesting potential market dynamics or operational limitations affecting power sales in these ranges. Moreover, the irregular fluctuations in frequency between 4 and 10 MW suggest shifts in market demand or VPP operational strategies. For instance, the decrease in the frequency of power sales between 6 and 7.5 MW, a sudden spike at 8 MW, and subsequent fluctuations may indicate market responses to pricing or supply dynamics, with the VPP adjusting its sales tactics accordingly. The peaks and valleys observed in the frequency distribution highlight the difficulties of optimizing power sales in response to evolving market conditions, varying demand, and operational factors. Ultimately, the frequency distribution provides valuable insights for enhancing the VPP's sales strategies, resource allocation, and market positioning to improve revenue generation and operational efficiency while effectively meeting market demand.

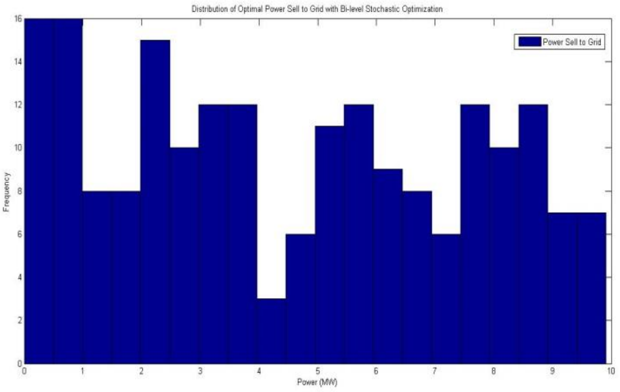

Fig. 19: Frequency distribution of power sold by VPP

V. Conclusion

In conclusion, the detailed analysis highlights the pivotal role of VPPs in modernizing and enhancing grid operations by integrating renewable energy sources such as PV systems, along with ESS, EVs, and HVAC systems. The study underscores the significant impact of factors like shading and weather uncertainties on solar power generation, emphasizing the need for advanced site selection, panel alignment, and forecasting methods to mitigate these effects. The analysis of ESS performance demonstrates that adaptive control strategies, particularly stochastic uncertainty management, are crucial for maintaining stable charging and SOC levels, improving both energy efficiency and system reliability. Similarly, EV charging demand responds dynamically to market influences and battery conditions, with adaptive control strategies further optimizing performance across different conditions. The case studies involving adaptive control strategy show the method's effectiveness in minimizing operational costs and maximizing power utilization, demonstrating how VPPs can enhance grid stability, reliability, and efficiency. Additionally, the application of bi-level stochastic optimization in VPP scheduling and bidding strategies proves to be a powerful approach, addressing uncertainties in the electricity market, improving decision-making processes, and maximizing revenue potential. By balancing risk and reward through probabilistic forecasting, this optimization framework enables VPPs to adapt to dynamic market conditions, enhancing both operational efficiency and economic resilience. Overall, this comprehensive analysis illustrates the transformative potential of VPPs in building a more sustainable, efficient, and reliable energy infrastructure capable of meeting the challenges of modern grid systems.

Acknowledgements

The authors would like to express their sincere gratitude to the School of Information Science and Engineering, Southeast University, Nanjing, China, and the Department of Electrical Engineering, Iqra National University, Peshawar, Pakistan, for providing the technical and academic support necessary for this research. Special thanks are extended to the reviewers and editors of the International Journal of Electrical Engineering and Applied Sciences for their constructive feedback, which helped improve the quality of this manuscript. The authors also acknowledge the use of relevant datasets, simulation tools, and computing resources that contributed to the successful completion of this study.

Conflict of Interest

The authors declare no conflict of interest in the publication process of the research article.

Author Contributions

Sajjad Khan: Conceptualization, Methodology, Formal analysis, Writing – Original Draft, Supervision.

M. Sajjad: Simulation, Data Curation, Visualization, Writing – Review & Editing.

A. Khan: Literature Review, Validation, Software Implementation.

M. Ikram: Investigation, Resources, Writing – Review & Editing.

M. Zafran: Project Administration, Funding Acquisition, Supervision.

References

[1]. Chadokar, L., Kirar, M.K., Yadav, G.K. et al. (2024). Aggregation and Bidding Strategy of Virtual Power Plant. *J. Electr. Eng. Technol*, https://doi.org/10.1007/s42835-024-02061-w

[2]. Zhongkai, Yi., Yinliang, Xu., Wei, Gu., Lun, Yang., Hongbin, Sun. (2021). Aggregate Operation Model for Numerous Small-Capacity Distributed Energy Resources Considering Uncertainty. IEEE Transactions on Smart Grid, doi: 10.1109/TSG.2021.3085885

[3]. Bomiao, Liang., Weijia, Liu., Lei, Sun., Zhiyuan, He., Beiping, Hou. (2019). An Aggregated Model for Energy Management Considering Crowdsourcing Behaviors of Distributed Energy Resources. IEEE Access, doi: 10.1109/ACCESS.2019.2945288

[4]. Yufan, Zhang., S., Dey., Yu-Yuan, Shi. (2023). Optimal Vehicle Charging in Bilevel Power-Traffic Networks via Charging Demand Function. arXiv.org, doi: 10.48550/arXiv.2304.11284

[5]. Beibei, Li., Yuqing, Guo., Qingyun, Du., Ziqing, Zhu., Xiaohui, Li., Rongxing, Lu. (2023). $\bm {P}^{\bm {3}}$: Privacy-Preserving Prediction of Real-Time Energy Demands in EV Charging Networks. IEEE Transactions on Industrial Informatics, doi: 10.1109/TII.2022.3182972

[6]. Shiping, Shao., Hossein, Sartipizadeh., Abhishek, Gupta. (2023). Scheduling EV Charging Having Demand With Different Reliability Constraints. IEEE Transactions on Intelligent Transportation Systems, doi: 10.1109/tits.2023.3279070

[7]. Jiarui, Wang., Jun, Leng., Jiajun, Zhang., Xue-jun, Chang. (2023). Charging and Discharging Scheduling Optimization Method of Electric Vehicle Based on User Demand Response Ability. doi: 10.1109/ACPEE56931.2023.10135684

[8]. Bin, Li., Bing, Qi., Yi, Sun., Liangrui, Tang., Huaguang, Yan. (2014). An Efficient Networked HVAC Controlling System by Using Multi-Mode Concentrator P-Cycle. Journal of Internet Technology, doi: 10.6138/JIT.2014.15.3.05

[9]. Jun, Zhang., Kan, Yu, Zhang. (2011). An Improved Particle Swarm Optimization Approach for Temperature Control in HVAC for the Purpose of Energy Saving. Advanced Materials Research, doi: 10.4028/WWW.SCIENTIFIC.NET/AMR.383-390.4768

[10]. Sumaiya, Tasnim., Nasser, Hosseizadeh., Apel, Mahmud., Ameen, Gargoom. (2020). How VPPs Facilitate the Integration of Renewable Energy Sources in the Power Grid and Enhance Dispatchability - A Review.

[11]. Nila, Thaker., Riaz, K., Israni. (2021). Integration of IEEE 14 Bus with Solar PV and VSG Systems. International Journal of Advance Research and Innovative Ideas in Education,

[12]. Jiayi, Liu. (2023). Particle swarm algorithm based microgrid dispatch optimization. doi: 10.1109/ICETCI57876.2023.10176670

[13]. Ghulam, Abbas., Aqeel, Ahmed, Bhutto., Touqeer, Ahmed, Jumani., Sohrab, Mirsaeidi., M., A., Tunio., Hammad, Alnuman., Ahmed, Alshahir. (2022). A Modified Particle Swarm Optimization Algorithm for Power Sharing and Transient Response Improvement of a Grid-Tied Solar PV Based A.C. Microgrid. Energies, doi: 10.3390/en16010348.